Journal of Nuclear Materials 390–391 (2009) 408–411

Contents lists available at ScienceDirect

Journal of Nuclear Materials

journal homepage: www.elsevier.com/locate/jnucmat

Simulation of H-modes discharges in ASDEX-Upgrade and MAST

V. Rozhansky [a], E. Kaveeva [a,*], P. Molchanov [a], I. Veselova [a], S. Voskoboynikov [a], D. Coster [b], G. Counsell [c], A. Kirk [c], S. Lisgo [c], ASDEX-Upgrade Team

[a] St. Petersburg State Polytechnical University, Polytechnicheskaya 29, 195251 St. Petersburg, Russia
[b] Max-Planck Institut für Plasmaphysik, EURATOM Association, Garching, Germany
[c] EURATOM/UKAEA Fusion Association, Culham Science Centre, Abingdon, Oxon OX14 3DB, UK

ARTICLE INFO

PACS:
52.25.Fi
52.55.Fa
52.65.Kj

ABSTRACT

A new version of the B2SOLPS5.0 transport code, which is free from numerical problems in the barrier region, has been used to simulate H-mode shots from ASDEX-Upgrade and MAST. The radial electric field inside the edge transport barrier and in the pedestal region is close to the neoclassical prediction. The shear of poloidal $\vec{E} \times \vec{B}$ drift at the inner side of the barrier is close to the value before the transition, while inside the barrier it is significantly larger. It is demonstrated that to match the experimental density and temperature radial profiles the drop in the diffusion coefficient within the barrier should be significantly larger than the drop in the electron heat conductivity.

1. Introduction

In recent years many simulations have been performed for Ohmic discharges of several tokamaks using the B2SOLPS5.0 fluid code [1–3]. In the equation system used in B2SOLPS5.0 [4], as well as in the UEDGE [5] and EDGE2D [6] codes, the divergent free parts of diamagnetic drifts in the parallel momentum balance, particle and energy balances were eliminated. The radial particle and energy fluxes corresponding to ∇B driven guiding center drifts were introduced. The divergence of these fluxes is the same as the divergence of the diamagnetic fluxes. The numerical scheme, based on these equations, was quite satisfactory for the simulation of Ohmic shots.

However, simulation of H-mode discharges, when the transport coefficients are reduced by an order of magnitude inside the barrier, is much more complicated. Firstly, the convergence of the numerical scheme is much worse in this situation. Secondly, the diffusion coefficient inside the barrier requires a numerical correction, in order to provide numerical stability $D^{corrected} = \sqrt{D^2 + (hV)^2}$ where h is the width of a numerical cell and V is convective velocity. Artificial diffusion, which is proportional to the local convective flow, in the presence of large radial ∇B driven convective fluxes in the upper and lower parts of flux surface becomes comparable with the real diffusion. As a consequence, the radial density profile can be calculated incorrectly.

To overcome these problems a new equation system has been implemented where strong radial particle and energy convective fluxes have been replaced by poloidal fluxes with the same divergence. On the closed flux surfaces, where the ion pressure is almost constant, the poloidal projection of the new velocity is similar to the poloidal projection of the parallel Pfirsch–Schlueter velocity. The radial component of the new velocity is rather small, so that the radial convective flux is also small. So physically we have replaced the divergence of the diamagnetic flux by the divergence of the Pfirsch–Schlueter flux. The electron and ion ∇B-drift heat fluxes were transformed in a similar way in order to decrease the radial convective heat fluxes. The new equation system is equivalent to the previous one but has better convergence.

An additional problem of H-mode simulations is the high plasma temperatures in the pedestal region. The inner side of the simulation domain usually corresponds to the plateau or even banana regimes. The radial electric field and neoclassical contribution to radial heat flows are calculated in the code B2SOLPS5.0 self-consistently through the parallel momentum balance and heat balance including diamagnetic and Pfirsch–Schlueter heat flows. To provide the correct neoclassical radial net heat flow and radial electric field, the parallel viscosity coefficient corresponding to viscosity associated with heat flow in the momentum balance and ion heat transport coefficients were modified accordingly. It is known from neoclassical theory that fluid description with these coefficients gives the same radial electric field as rigorous kinetic treatment.

Several H-mode shots for ASDEX-Upgrade (AUG) and MAST were simulated using the new version of the code. Results of the simulations are presented and discussed below.

* Corresponding author.
E-mail address: kaveeva@edu.ioffe.ru (E. Kaveeva).

0022-3115/$ - see front matter © 2009 Elsevier B.V. All rights reserved.
doi:10.1016/j.jnucmat.2009.01.101

2. Simulation of ASDEX-Upgrade and MAST H-mode shots

Simulations have been performed for AUG H-mode shot #17151 and MAST H-mode shot #17469. The density and temperature profiles at the equatorial mid-plane from the simulations and the experiment [7] are shown in Fig. 1(a)–(c) and Fig. 2(a) and (b). The radial profiles of the transport coefficients in the simulations are presented in Fig. 3. As seen from Fig. 3, to match the experimentally observed radial profiles the turbulent diffusion coefficient has to be reduced by a factor of ten inside the transport barrier while the reduction of the electron heat conductivity is only a factor of two. This fact is typical both for AUG and MAST. In Fig. 3(a) the effective neoclassical ion heat conductivity calculated with the code NEOART [8] is plotted. The neoclassical heat conductivity is quite big, of the same order as the turbulent heat conductivity both in the core and inside the barrier. Examples of comparison of measured and simulated plasma parameters near the divertor plates are shown in Figs. 4 and 5.

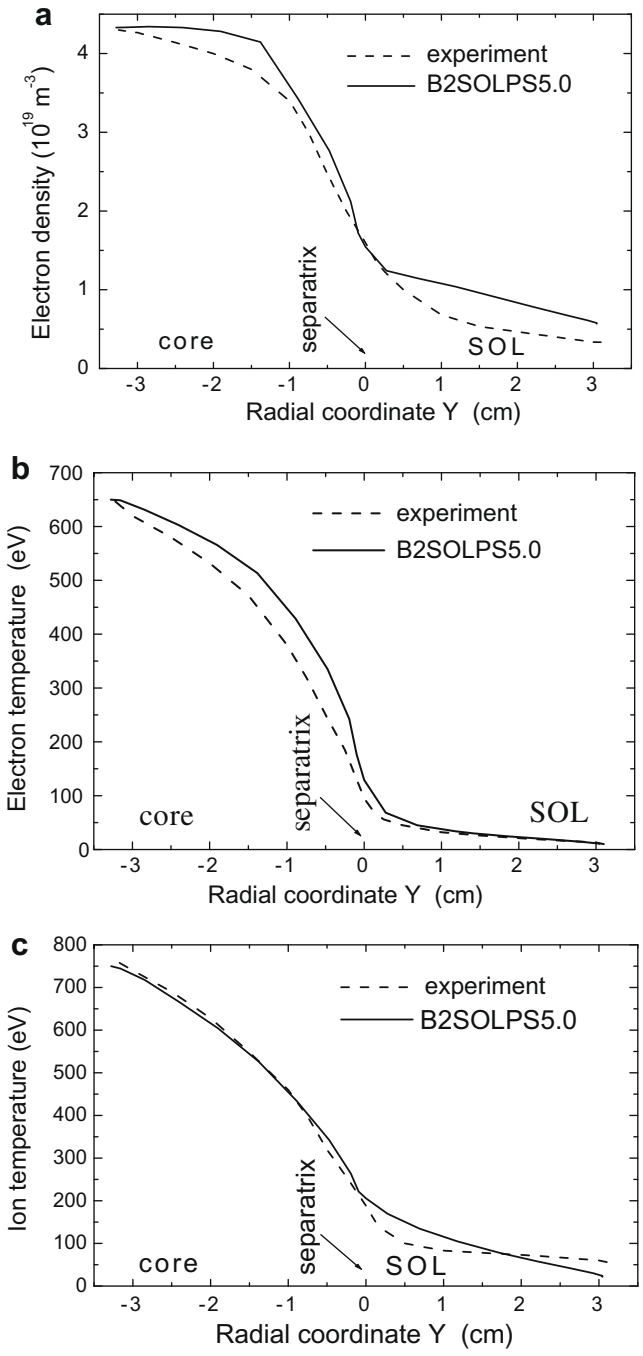

Fig. 1. Radial profiles at the outer mid-plane for AUG shot #17151: (a) electron density; (b) electron temperature; (c) ion temperature.

The radial electric field from the simulations has been compared to the neoclassical electric field calculated using the expression:

$$E^{(NEO)} = \frac{T_i}{e}\left(\frac{1}{h_y}\frac{d\ln n}{dy} + k^T\frac{1}{h_y}\frac{d\ln T_i}{dy}\right) - b_x\frac{\oint\sqrt{g}V_{||}Bdx}{\oint\sqrt{g}dx}, \quad (1)$$

where k^T is taken according to [9]. The comparison is shown in Figs. 6 and 7 where it can be seen that the simulations for both AUG and MAST agree well with the neoclassical values.

3. Issues of edge transport barrier physics

In H-mode the parallel velocity in the SOL and inside the transport barrier are significantly larger than in the L-mode discharges. For example, the maximal values of the parallel velocity at the outer mid-plane are 60 km/s in AUG and 30 km/s in MAST, Fig. 8, while characteristic values for AUG L-regimes are 6–10 km/s [10]. The Mach numbers in the H-mode shots both for AUG and for MAST are of the order of 0.3–0.4 very near the separatrix.

The width of the transport barrier Δ can be estimated self-consistently through the critical value ω_0 of the shear ω_s, corresponding to the L–H transition. As can be seen from the modeling, the radial electric field in the barrier is approximately neoclassical. Its value can be estimated as $E_r \approx \frac{T_i}{eL_n}$, where $L_n = |\frac{1}{n}\frac{dn}{h_y dy}|^{-1}$ is of the order of Δ. The shear of the $\vec{E}\times\vec{B}$ drift $\omega_s = \frac{RB_x}{B}|\frac{d(E_y/B_xR)}{h_y dy}|$ can be estimated as $\omega_s \approx \frac{E_r}{B\Delta}$. The shear value in the barrier should be bigger than ω_0, so an estimate for the width of the transport barrier is $\Delta \approx \sqrt{\frac{T_i}{e\omega_0 B}}$. Taking $\omega_0 = 5\times10^5$ s^{-1}, $T_i = 300$ eV, $B = 2T$ for AUG, the value $\Delta \approx 1.7$ cm is obtained, which is similar to the experimental width of the transport barrier.

In previous simulations [1–3] it has been shown that the L–H transition takes place when the shear of $\vec{E}\times\vec{B}$ drift reaches a value $\omega_s = \omega_0 = 3\times10^5$–$10^6$ s^{-1}, which is the same order as the value that determines the pedestal width. However, (ρ_{ci} is the ion gyroradius) $\omega_s \sim \frac{c_s}{L_n}\frac{\rho_{ci}}{L_n}$, which is much smaller than the drift wave frequency for $k_\perp\rho_{ci}\sim 1$: $\omega_d \sim c_s/L_n$. It is possible that the shear influences the long wavelength part of the spectrum; some supporting results can be found in the simulations performed with a turbulence code [11]. The parametric dependence of ω_0 is not understood at present and hence it is difficult to predict the parametric dependence for the barrier width on the basis the estimate.

In order to match the experimental profiles in both MAST and AUG, the drop of the diffusion coefficient inside the barrier is ~10, while the drop in the electron heat conductivity coefficient is ~2 or less. This might be an indication of the fact that the particle diffusivity is determined by the large scale turbulence which is suppressed by the shear of $\vec{E}\times\vec{B}$ drift. The anomalous ion heat conductivity might also be governed by the same turbulence, and might be also suppressed. However, it is difficult to estimate the level of its suppression because it is masked by the large heat conductivity caused by ion-neutral collisions. On the contrary the fact that the electron heat conductivity coefficient is only modestly suppressed within the barrier is rather robust. The possible explanation is that the electron heat conductivity is determined by the small scale turbulence which survives during the process of the shear suppression. Still the question remains which type of turbulence is responsible for electron heat conductivity. Very different diffusion and electron heat conductivity coefficients are typical for magnetic flutter, but at present there is no direct evidence of this process.

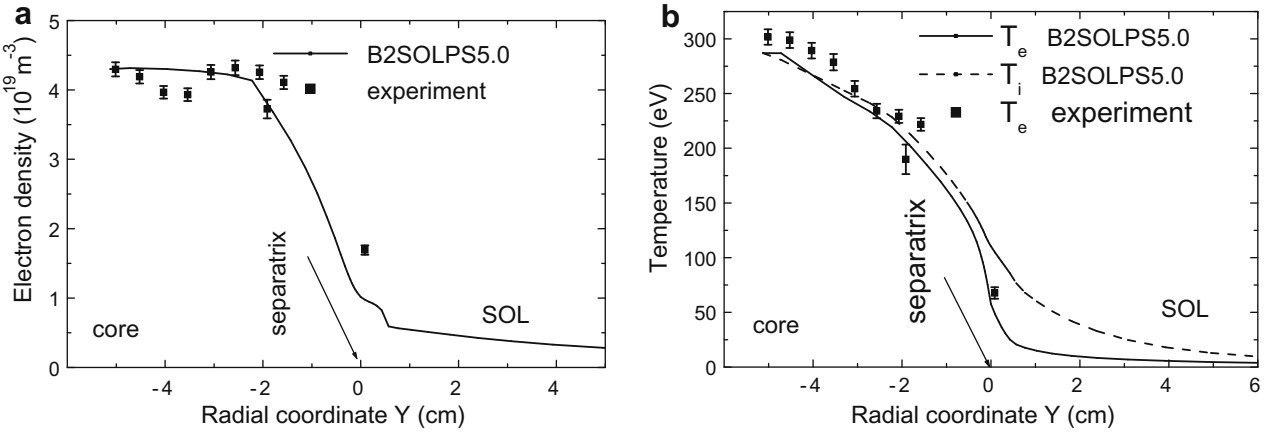

Fig. 2. Radial profiles at the outer mid-plane for MAST shot #17469: (a) electron density; (b) electron temperature.

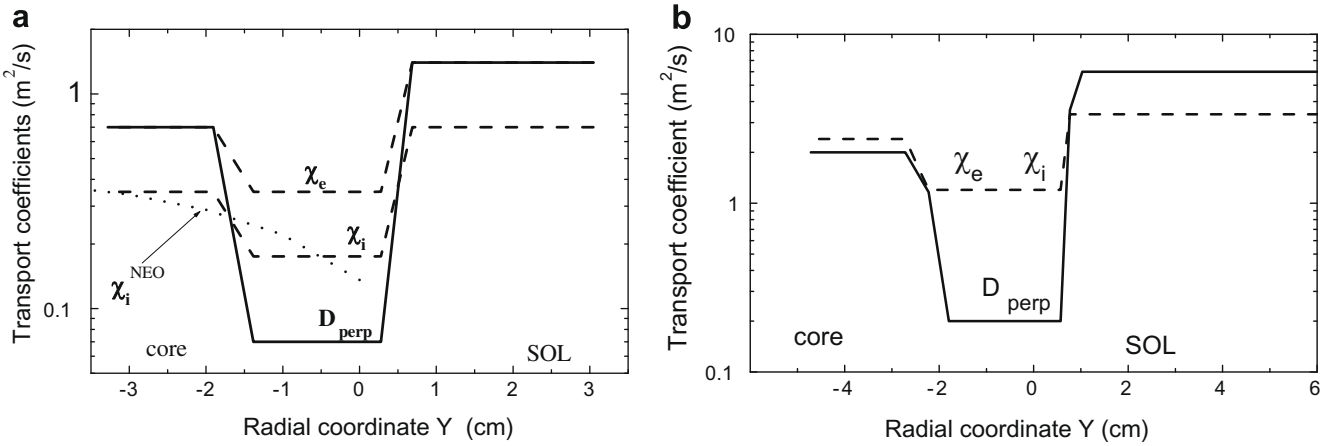

Fig. 3. Radial profiles of anomalous transport coefficients at the outer mid-plane chosen for simulations: (a) AUG shot #17151; (b) MAST shot #17469.

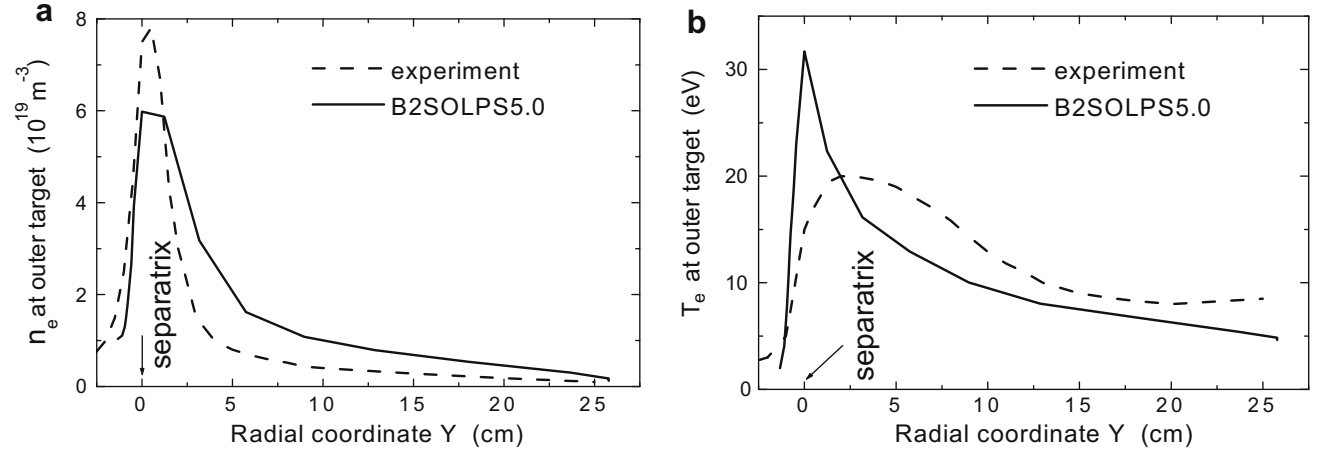

Fig. 4. Profiles at the outer divertor plate for AUG shot #17151: (a) electron density; (b) electron temperature.

4. Conclusions

A new version of the B2SOLPS5.0 transport code has been developed and implemented for the simulation of H-mode shots from ASDEX-Upgrade and MAST. It is demonstrated that the diffusion coefficient inside the barrier is reduced by a factor of 10 with respect to the L-mode value, while the electron heat conductivity coefficient is reduced by a factor of 2 or less. The radial electric field inside the separatrix is close to the neoclassical electric field as in L-mode. The toroidal rotation is co-current directed as in L-mode but is significantly larger in absolute value. The shear of the poloidal $\vec{E} \times \vec{B}$ drift at the pedestal is close to the value of the shear be-

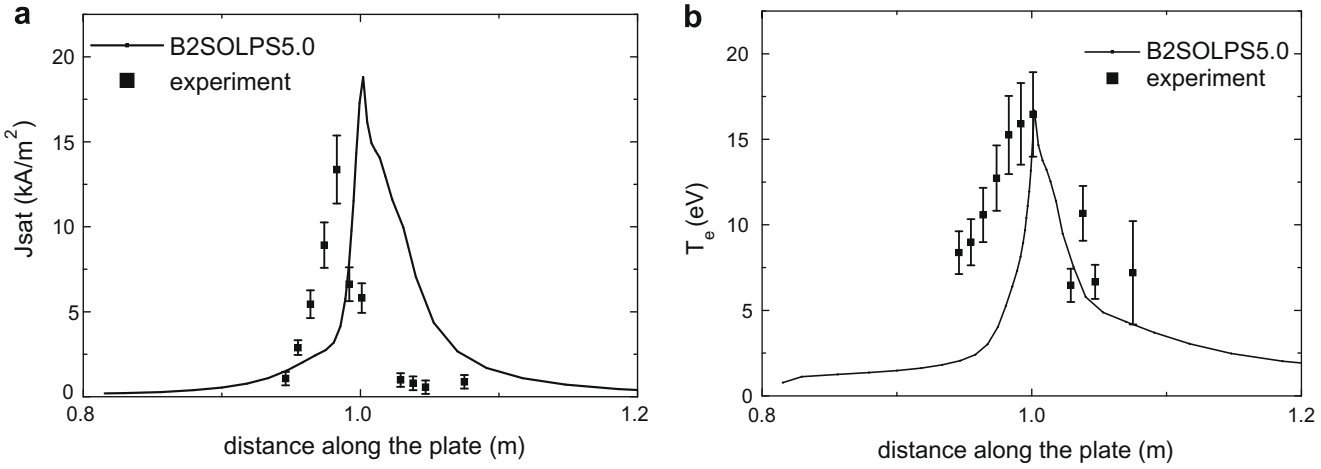

Fig. 5. Profiles at the outer lower divertor plate for MAST shot #17469: (a) saturation current; (b) electron temperature.

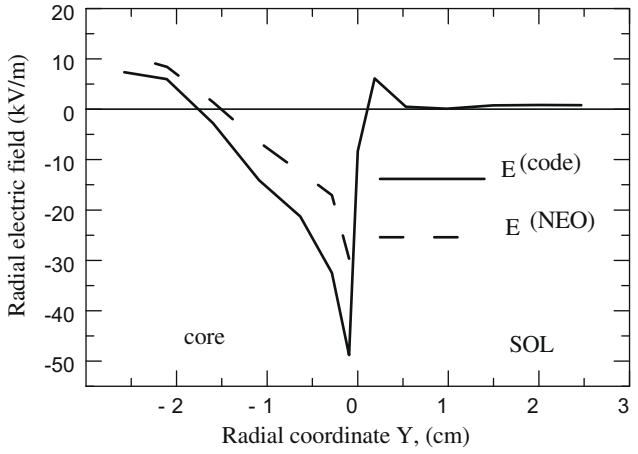

Fig. 6. Calculated radial electric field at the outer mid-plane for AUG shot #17151.

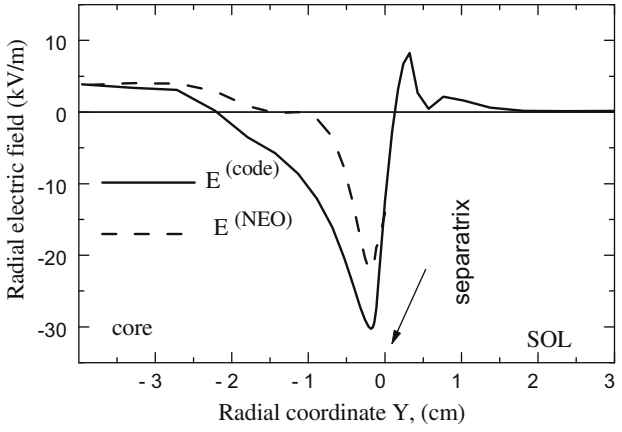

Fig. 7. Calculated radial electric field at the outer mid-plane for MAST shot #17469.

fore the L–H transition, while inside the barrier the value of the shear is significantly larger.

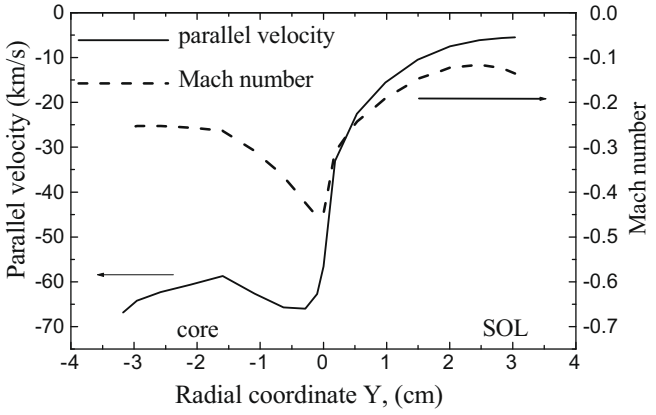

Fig. 8. Calculated parallel velocity at the outer mid-plane for AUG shot #17151.

Acknowledgements

The work was supported by Grant RFFI no. 06-02-16785. The authors are grateful to C. Konz for providing the results of the NEO-ART simulations. UKAEA authors were funded jointly by the United Kingdom Engineering and Physical Sciences Research Council and by the European Communities under the contract of Association between EURATOM and UKAEA. The views and opinions expressed herein do not necessarily reflect those of the European Commission.

References

[1] V. Rozhansky, Plasma Phys. Control. Fus. 46 (2004) A1.
[2] V. Rozhansky, Contribution Plasma Phys. 46 (2006) 575.
[3] R. Schneider et al., Contribution Plasma Phys. 46 (2006) 3.
[4] V. Rozhansky, S. Voskoboynikov, E. Kaveeva, D. Coster, R. Schneider, Nucl. Fus. 41 (2001) 387.
[5] T.D. Rognlien, Plasma Phys. Control. Fus. 47 (2005) A283.
[6] G.J. Radford et al., Contribution Plasma Phys. 36 (2/3) (1996) 187.
[7] L.D. Horton et al., Nucl. Fus. 45 (2005) 856.
[8] A.G. Peeters, Phys. Plasmas 7 (2000) 1721.
[9] F.L. Hinton, R.D. Hazeltine, Rev. Mod. Phys. 48 (1976) 239.
[10] V. Rozhansky et al., Contribution Plasma Phys. 48 (2008) 73.
[11] B. Scott, Plasma Phys. Control. Fus. 48 (2006) A387.